

Plasma density measurements on COMPASSC tokamak from electron cyclotron emission cutoffs

D. Chenna Reddy and T. Edlington

Citation: *Rev. Sci. Instrum.* **67**, 462 (1996); doi: 10.1063/1.1146613

View online: <http://dx.doi.org/10.1063/1.1146613>

View Table of Contents: <http://rsi.aip.org/resource/1/RSINAK/v67/i2>

Published by the [American Institute of Physics](http://www.aip.org).

Related Articles

Spherical torus equilibria reconstructed by a two-fluid, low-collisionality model

[Phys. Plasmas](#) **19**, 102512 (2012)

Oblique electron-cyclotron-emission radial and phase detector of rotating magnetic islands applied to alignment and modulation of electron-cyclotron-current-drive for neoclassical tearing mode stabilization

[Rev. Sci. Instrum.](#) **83**, 103507 (2012)

Toroidal rotation of multiple species of ions in tokamak plasma driven by lower-hybrid-waves

[Phys. Plasmas](#) **19**, 102505 (2012)

Perpendicular dynamics of runaway electrons in tokamak plasmas

[Phys. Plasmas](#) **19**, 102504 (2012)

Electron cyclotron current drive modelling with parallel momentum correction for tokamaks and stellarators

[Phys. Plasmas](#) **19**, 102501 (2012)

Additional information on Rev. Sci. Instrum.

Journal Homepage: <http://rsi.aip.org>

Journal Information: http://rsi.aip.org/about/about_the_journal

Top downloads: http://rsi.aip.org/features/most_downloaded

Information for Authors: <http://rsi.aip.org/authors>

ADVERTISEMENT

ORTEC MAESTRO[®] V7 MCA Software

For over two decades, MAESTRO has set the standard for Windows-based MCA Emulation. MAESTRO Version 7.0 advances further:

- New!** Windows 7 64-Bit Compatibility with Connections Version 8
- New!** List Mode Data Acquisition for Time Correlated Spectrum Events
- New!** Improved Peak fit calculations
- New!** Improved graphics handling for multiple displays
- New!** Open spectrum files directly from Windows Explorer
- New!** Improved performance with Job Functions and display updates

MAESTRO continues to be the world's most popular nuclear MCA software in a broad range of applications!



**Now 64-bit
Windows 7
Compatible!**

www.ortec-online.com

Plasma density measurements on COMPASS-C tokamak from electron cyclotron emission cutoffs

D. Chenna Reddy^{a)} and T. Edlington

UKAEA Fusion/Euratom Association, Culham Laboratory, Abingdon, Oxon, OX14 3DB, United Kingdom

(Received 22 June 1993; accepted for publication 24 October 1995)

Electron cyclotron emission (ECE) is a standard diagnostic in present day tokamak devices for temperature measurement. When the plasma density is high enough the emission at some frequencies is cut off. Of these cutoff frequencies, the first frequency to cut off depends on the shape of the density profile. If the density profile can be described by a few parameters, in some circumstances, this first cutoff frequency can be used to obtain two of these parameters. If more than two parameters are needed to describe the density profile, then additional independent measurements are required to find all the parameters. We describe a technique by which it is possible to obtain an analytical relation between the radius at which the first cutoff occurs and the profile parameters. Assuming that the shape of the profile does not change as the average density rises after the first cutoff, one can use the cutoffs at other frequencies to obtain the average density at the time of these cutoffs. The plasma densities obtained with this technique using the data from a 14 channel ECE diagnostic on COMPASS-C tokamak are in good agreement with those measured by a standard 2 mm interferometer. The density measurement using the ECE cutoffs is an independent measurement and requires only a frequency calibration of the ECE diagnostic. © 1996 American Institute of Physics. [S0034-6748(96)00302-8]

I. INTRODUCTION

Electron cyclotron emission (ECE) diagnostics are routinely used for plasma temperature and its fluctuation measurements in many present day tokamak experiments.¹⁻⁶ The use of multichannel superheterodyne receivers has made it possible to measure this emission with good spatial and temporal resolution.^{7,8} However, the range of usefulness of ECE as a temperature diagnostic is limited by cutoffs and resonances occurring in the plasma and by the plasma optical thickness. O-mode emission will be cut off, i.e., not observed, if the plasma frequency is greater than the emission frequency anywhere between the emitting surface and the observation point (antenna). For the X-mode emission the right- and left-hand cutoff frequencies⁹ determine whether the emission is cut off. Since these cutoff frequencies depend on the plasma density, one can use the observation of cut off as a local density measurement. The frequency calibration needed to calculate the cutoff density and its radial location is known to better than 0.2 GHz. If we can neglect the poloidal magnetic field, the other information required is the toroidal magnetic field, which is well known. Since no other information is required, this is an independent measurement which can be compared with other diagnostic measurements.

In order to use the observation of a cutoff as a density measurement one not only needs to know what emission frequency is cut off but also where the cutoff actually occurs. In some circumstances it is possible to find this location which then enables one to determine the density at the cutoff location at the time of the observation of a cutoff. At low densities, the cutoff frequency is low and the emission does not encounter any cutoff on its propagation to the receiver.

As the density rises the cutoff frequency increases and eventually emission at some frequencies will be cut off. The frequency at which the emission cuts off *first* depends on the shape of the density profile. For broad density profiles the frequency to cut off first occurs nearer to the outer edge of the plasma and for peaked profiles the frequency closer to the center of the plasma cuts off first. Thus the peakedness of the profile determines which frequency cuts off first. This dependence of the *first* frequency to cut off on the profile shape can be used in some circumstances to obtain two of the parameters describing the profile at the time of the first cutoff. If the profile description needs more than two parameters, then additional independent measurements are required to determine all the parameters. If the density is falling during its evolution, then the last frequency to cut on can be used to determine these parameters.

This type of technique was first used by Lohr¹⁰ on DIII-D tokamak to infer the plasma density profile shape. The method involved determining the tangency of the right-hand cutoff frequency and the second harmonic of the cyclotron frequency when plotted as a function of radius. This tangency point is found empirically to an accuracy which is three times less than the resolution of the ECE system. In this paper we derive an analytical relation between the profile parameters and the radius at which emission is first cut off. The accuracy to which the profile parameters can be determined therefore depends only on the resolution of the ECE system. Also, the analytical procedure presented in this paper can be applied to a more general class of profiles than the one considered by Lohr.¹⁰ We describe the principle of this method in Sec. II. In Sec. III we present the results of applying this method to data obtained on COMPASS-C tokamak and compare them with an independent measurement of the line average density. Some practical considerations are discussed in Sec. IV.

^{a)}Permanent address: Institute for Plasma Research, Bhat, Gandhinagar-382 424, India.

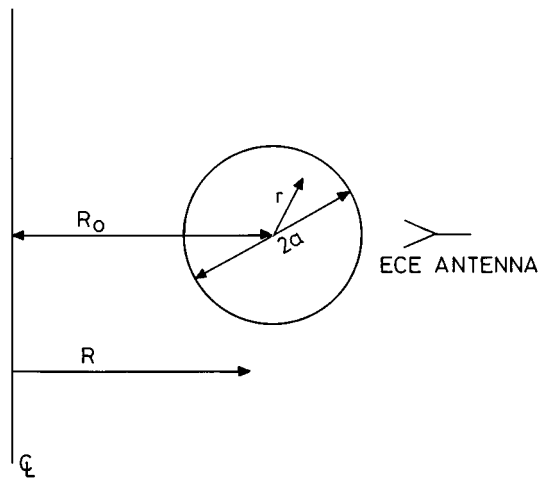


FIG. 1. Schematic of the geometry showing the antenna location.

II. PRINCIPLE OF THE METHOD

We consider X -mode emission at the second-harmonic electron cyclotron frequency, $2f_{ce}$, and assume that the emission from the equatorial plane is received perpendicular to the toroidal magnetic field by an antenna on the low field side of the tokamak as shown in Fig. 1. Here, R_0 and a are the major and minor radii of the plasma, respectively. The distances from the major axis and the plasma center are denoted by R and r , respectively. Emission will be cut off if the right-hand cutoff frequency, f_r , is greater than or equal to $2f_{ce}$ (evaluated at the emitting position) anywhere between the emitting position and the receiving antenna. The equality holds when the cutoff “just” occurs. We define a particular frequency to be *locally* cut off if that frequency is first cut off by the right-hand cutoff frequency evaluated at the same position as that of the emitting frequency.

For density profiles symmetric about $r=0$, the first frequency to be cut off as the density increases is always on the low field side of the tokamak and will be $\leq 2f_{ce}(R_0)$. Further, if the density is a monotonically decreasing function of r , all the frequencies smaller than $2f_{ce}(R_0)$ which are cut off will be cut off locally. For the purpose of this paper we consider only those density profiles which are symmetric and monotonically decreasing functions of r . We also assume that the functional form describing the density profile does not change during the observation of cutoffs at various frequencies. That is, the ratio of the plasma densities at any two spatial points remains the same during this time.

Figure 2 shows the right-hand cutoff frequency for a parabolic density profile for the COMPASS-C tokamak ($R_0=55.7$ cm and $a=19.6$ cm) at three different central densities along with the cyclotron frequency and its second harmonic as a function of the distance from the major axis, R . Curve (a) shows the right-hand cutoff frequency when the first cut off occurs. Curve (b) is when the *maximum* of the right-hand cutoff frequency is equal to the second-harmonic cyclotron frequency at the same radial location. This location is found to be at $R=52.14$ cm for this case. As the density rises further, the maximum of the right-hand cutoff frequency moves toward the center of the plasma. Since the

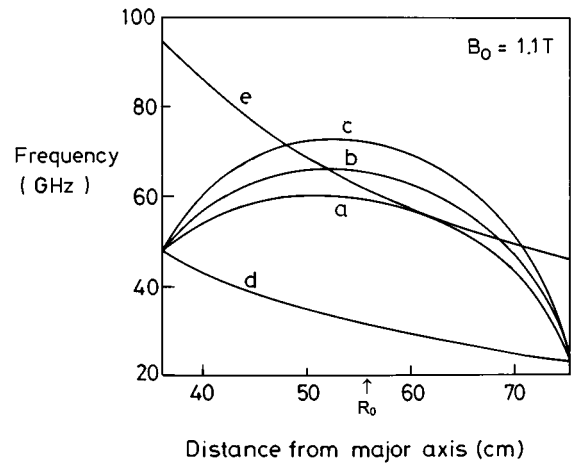


FIG. 2. Right-hand cutoff frequency, f_r , for a parabolic density profile at three different central densities: curves (a), (b), and (c); and cyclotron frequency, f_{ce} , and its second harmonic, $2f_{ce}$: curves (d) and (e) as a function of distance from the major axis.

emission from locations to the left of $R=52.14$ cm will be cut off at the maximum of f_r first, they are not *local* cutoffs according to our above definition. Thus the emission frequency at $R=52.14$ cm is the highest frequency to cut off locally. This is not necessarily the last frequency to cut off locally, as can be seen from Fig. 2. There will be some more frequencies to the right of the right-hand side intersection of $2f_{ce}$ and f_r , yet to be cut off and will be cut off locally as the density further rises. Curve (c) corresponds to the situation where some of the frequencies are not local cutoffs. Curves (d) and (e) are the cyclotron frequency and its second harmonic, respectively.

In the cold plasma approximation the right-hand cutoff frequency is given by⁹

$$f_r = \frac{1}{2} [f_{ce} + \sqrt{f_{ce}^2 + 4f_{pe}^2}], \quad (1)$$

where f_{pe} is the electron plasma frequency. As the plasma density increases, the right-hand cutoff frequency increases and eventually cyclotron emission becomes cut off, first at a single frequency and later at lower and higher frequencies. The frequencies which cut off locally satisfy the relation:

$$f_r(R) = 2f_{ce}(R). \quad (2)$$

Substituting $2f_{ce}$ for f_r in Eq. (1), we get the following condition for a local cutoff:

$$f_{pe}^2(R) = 2f_{ce}^2(R). \quad (3)$$

Noting that $f_{pe} = 8.98 \times \sqrt{n_e}$ Hz, where n_e is the plasma density in m^{-3} , we can write Eq. (3) as

$$n_e(r) = \frac{2f_{ce}^2(R)}{80.64}, \quad (4)$$

where $R=R_0+r$. Equation (4) gives the density needed at r for the emission to be locally cut off. When we observe the first cutoff, which is a local cutoff, we assume that the density can be parametrized by

$$n_e(r) = n_e(0)(1 - r^2/a^2)^\alpha, \quad (5)$$

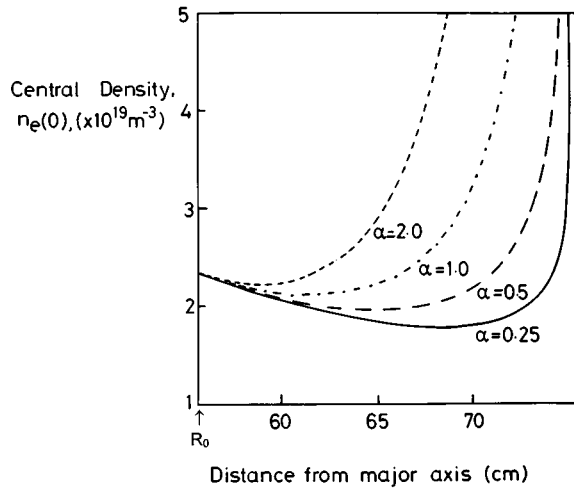


FIG. 3. Central density, $n_e(0)$, required for a local cutoff at R from Eq. (6) as a function of R for different values of the profile parameter, α .

where the central density, $n_e(0)$, and the profile parameter, α , are free parameters. As noted in Ref. 10, it is not possible to determine both $n_e(0)$ and α from the observed cutoff using only Eq. (5). However, combining Eqs. (4) and (5) and using the $1/R$ dependence of $f_{ce}(R)$, we obtain the following equation for the central density, $n_e(0)$, for which a local cutoff occurs at $R(=R_0+r)$:

$$n_e(0) = \frac{1.94 \times 10^{19} B_0^2}{(1+r/R_0)^2}, \quad (6)$$

where B_0 is the toroidal magnetic field in tesla at R_0 . A plot of $n_e(0)$ as a function of R is shown in Fig. 3 for different values of α . These curves show a minimum in $n_e(0)$ at different radii for different values of α . For a constant value of α , as $n_e(0)$ increases the radius at which the emission cuts off first is that at which $n_e(0)$ is minimum in Fig. 3. Also from Fig. 3 we can see that the higher the value of α , the closer to the plasma center the first cutoff occurs. Since $n_e(0)$ has a minimum, from Eq. (6) we get

$$\left[\frac{d}{dr} [n_e(0)] \right]_{r=r_{fco}} = \frac{d}{dr} \left[\frac{1.94 \times 10^{19} B_0^2}{(1+r/R_0)^2 (1-r^2/a^2)^\alpha} \right]_{r=r_{fco}} = 0, \quad (7)$$

where r_{fco} is the radius at which the first cutoff occurs. For a nontrivial solution of Eq. (7)

$$\alpha = \frac{a^2 - r_{fco}^2}{r_{fco}^2 + r_{fco} R_0}. \quad (8)$$

This equation uniquely determines the value of α from the first cutoff radius, r_{fco} . We may note that this relation between α and r_{fco} does not depend on B_0 . A plot of α as a function of the first cutoff position is shown in Fig. 4. Having obtained a value for α from the first cutoff radius, $n_e(0)$ can be deduced from Eq. (6). Using these values of α and $n_e(0)$ the average density can be calculated when the first cutoff occurs. Assuming that α remains constant during the

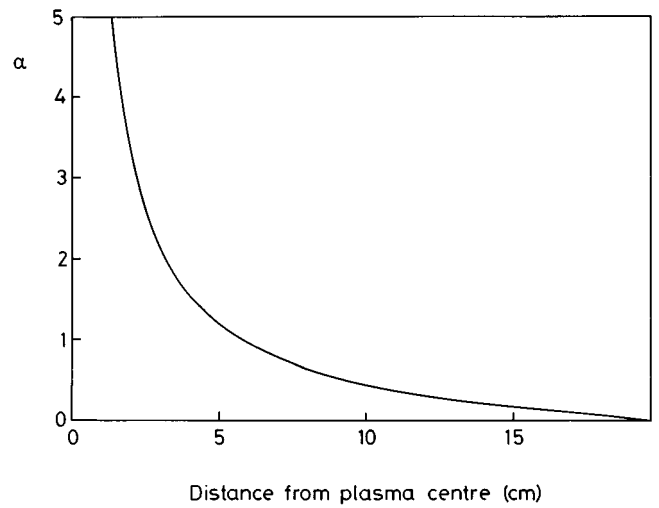


FIG. 4. Variation of the profile parameter, α , with the location of the first cutoff (measured from the plasma center).

density rise, one can calculate the average density at later times as more and more frequencies are cut off, provided they are *locally* cut off.

The maximum of the right-hand cutoff frequency occurs at a location $\leq R_0$. This maximum moves toward R_0 as the density rises. When this maximum, $f_r(R_m)$, equals the emission frequency at the same location, $2f_{ce}(R_m)$, the emission will be cut off locally. The emission frequencies higher than $2f_{ce}(R_m)$ when cut off will be cut off at the maximum of f_r and hence will be nonlocal cutoffs. Therefore $2f_{ce}(R_m)$ is the highest frequency to cut off locally, the location of which can be found as follows. At the maximum of f_r , we have

$$\left[\frac{df_r(R)}{dR} \right]_{R=R_m} = \frac{d}{dR} \left[\frac{f_{ce}(R)}{2} + \frac{1}{2} \sqrt{f_{ce}^2(R) + 4f_{pe}^2(R)} \right]_{R=R_m} = 0. \quad (9)$$

Since the location of this maximum, $R_m(=R_0-r_m)$, always occurs to the left of R_0 , $df_{pe}/dR = \alpha r f_{pe}/(a^2-r^2)$. Substituting this expression for df_{pe}/dR and $-f_{ce}/R$ for df_{ce}/dR in the above equation, we get

$$\frac{f_{ce}(R_m)}{R_m} \sqrt{f_{ce}^2(R_m) + 4f_{pe}^2(R_m)} = \frac{4\alpha r f_{pe}^2(R_m)}{a^2 - r_m^2} - \frac{f_{ce}^2(R_m)}{R_m}. \quad (10)$$

As the emission at this location is cut off locally, we can substitute $2f_{ce}^2(R_m)$ for $f_{pe}^2(R_m)$ from Eq. (3) in Eq. (10) to obtain the following quadratic equation in R_m :

$$(1-2\alpha)R_m^2 + 2R_0(\alpha-1)R_m + (R_0^2 - a^2) = 0. \quad (11)$$

One of the two roots of the above equation corresponds to the location of the maximum. The other root is unphysical and hence ignored. The location of the highest local cutoff frequency can then be written as

$$R_m = \frac{(1-\alpha)R_0 - \sqrt{\alpha^2 R_0^2 + a^2(1-2\alpha)}}{1-2\alpha}. \quad (12)$$

For $\alpha=0.5$, from Eq. (11) we get $R_m = (R_0^2 - a^2)/R_0$.

Frequencies which are cut off but not locally cut off can also be used to deduce the mean density at the time when the cutoff occurs, but in this case the calculation is more indirect. Any frequency, $2f_{ce}(R_1)$, higher than the highest frequency that is locally cut off, is cut off first when the maximum of the right-hand cutoff frequency, f_r , becomes equal to the emission frequency, $2f_{ce}(R_1)$ [see curve (c) in Fig. 2]. Since the emission is cut off first at the maximum of the right-hand cutoff frequency, when we observe the emission cutoff we have

$$2f_{ce}(R_1) = f_r(R_0 - r_{co}), \quad (13)$$

where r_{co} , the distance from the center of the plasma on the high field side, is the location of the maximum of f_r and hence the cutoff. Combining Eqs. (10) (where R_m is replaced by $R_0 - r_{co}$) and (13) we get the following cubic equation, one of the three roots of which gives the location of the cutoff:

$$4\alpha r_{co}^3 - [(1 + 2\alpha)R_1 - 8\alpha R_0]r_{co}^2 + 2\alpha R_0(2R_0 - R_1)r_{co} - \alpha^2 R_1 = 0. \quad (14)$$

By choosing the root which occurs between R_1 and R_0 , where the emission is actually cut off, we can calculate the plasma density, $n_e(r_{co})$, from Eq. (13) (where the left-hand side is evaluated at R_1 and the right-hand side is evaluated at $R_0 - r_{co}$), which can be expressed as

$$n_e(r_{co}) = \frac{2f_{ce}^2(R_1)}{80.64} \left[2 - \frac{R_1}{(R_0 - r_{co})} \right]. \quad (15)$$

From the plasma density at r_{co} calculated using Eq. (15) and the value of α obtained from the first cutoff, the average density can be calculated for the frequencies which are not locally cut off. These results from local and nonlocal cutoffs can be used to compare with the density evolution measured by a microwave interferometer.

Alternatively, the emission frequencies [$\leq 2f_{ce}^2(R_0)$] which are locally cut off can be used to infer the density profile assuming the profile shape is not changing with time. In this case, no explicit functional form for the density profile needs to be assumed. Let us assume that $n_e(r_1, t_1)$ is the cutoff density at r_1 observed from the cutoff at time t_1 . If the profile form is not changing we can calculate the density, $n_e(r_2, t_1)$, from the cutoff density at r_2 at a different time, t_2 , from the relation

$$n_e(r_2, t_1) = n_e(r_2, t_2) \frac{\bar{n}(t_1)}{\bar{n}(t_2)}, \quad (16)$$

where $\bar{n}(t_1)$ and $\bar{n}(t_2)$ are the line average densities measured by the interferometer at t_1 and t_2 , respectively. Using Eq. (16), we can calculate the densities at different radii but at the same time from the observed cutoff densities and the average densities to obtain the profile. Frequencies which are not locally cut off cannot be used in this way, since in this case the form of the density profile must be assumed *a priori* in order to relate the local density to the radius at which the right-hand cutoff frequency exceeds the frequency of emission.

For O-mode fundamental cyclotron emission, the emission cutoff occurs at the plasma frequency. A similar analysis can be carried out and one gets exactly the same relation [Eq. (8)] between r_{fco} and α if the density at the time of first cutoff can be described by Eq. (5). For this case all the frequencies less than $f_{ce}(R_0)$ are locally cut off. The frequencies higher than this frequency are cut off first at the maximum of the plasma frequency which occurs at $r=0$. The cutoff of these frequencies will therefore give a value for the central plasma density directly at the time when each is cut off. The left-hand cutoff frequency which effects the X-mode emission is always less than the right-hand cutoff frequency at any given location. Therefore the emission will be first cut off by the right-hand cutoff frequency and the left-hand cutoff frequency is not useful for this kind of density measurement.

One can use the same procedure described in this section for finding the profile parameters for other more general profiles. For example, if we assume that the density profile can be described by

$$n_e(r) = n_e(0)(1 - r^\beta/a^\beta)^\alpha, \quad (17)$$

we can show that the relation between the parameters α and β and the first cutoff radius, r_{fco} , is given by

$$\alpha\beta = \frac{2(a^\beta - r_{fco}^\beta)}{(r_{fco}^\beta + r_{fco}^{\beta-1}R_0)}. \quad (18)$$

If we have an independent central density, $n_e(0)$, measurement such as from a Thomson scattering diagnostic when the first cutoff occurs, we can calculate α and β using Eqs. (17) and (18).

A more realistic profile is one where there is a finite edge density, $n_e(a)$. In this case, if we assume that the density profile is described by

$$n_e(r) = [n_e(0) - n_e(a)](1 - r^2/a^2)^\alpha + n_e(a), \quad (19)$$

then one can show that the profile parameter, α , is given by

$$\alpha = \frac{a^2 - r_{fco}^2}{r_{fco}^2 + r_{fco}R_0} \left(1 - \frac{n_e(a)(1 + r_{fco}/R_0)^2}{1.94 \times 10^{19} B_0^2} \right)^{-1}, \quad (20)$$

which reduces to Eq. (8) when $n_e(a) = 0$. If we have the edge density measurement at the time of the first cutoff, perhaps from a Langmuir probe, we can calculate the profile parameter, α , from the above equation.

III. RESULTS

COMPASS-C is a circular tokamak with major and minor radii of 55.7 and 19.6 cm, respectively. The maximum available toroidal field is 2.1 T on axis. More detailed information about the COMPASS tokamak is available elsewhere.¹¹ The COMPASS-C 14 channel ECE diagnostic is a heterodyne radiometer receiving X-mode cyclotron emission in the frequency range of 53.0–66.5 GHz. Each channel has a bandwidth of ± 0.5 GHz and the channel separation is about 1.0 GHz. In practice the maximum of these two determines the radial resolution and hence the resolution of the cutoff radii. Figure 5 shows the cyclotron emission signals as

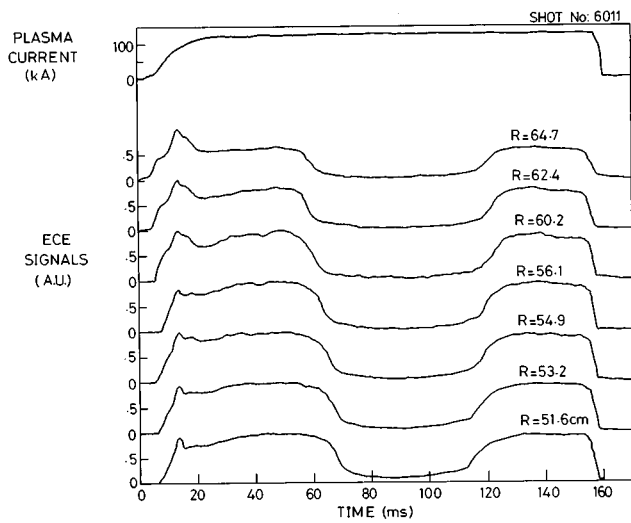


FIG. 5. Wave forms of plasma current, I_p , and ECE signals from some of the radiometer channels as a function of time. Each ECE channel is normalized to its own maximum value.

observed by some of the ECE channels along with plasma current for a shot where the plasma density was ramped up by gas puffing and then decreases when the gas puff is

switched off. The emission cutoff is seen in all the channels as the density rises. During the density fall emission reappears.

During the density rise the emission is first cut off in the channel corresponding to $R=62.4$ cm. Using Eq. (8) the value of α calculated is 0.81. During the density fall the emission which reappears last is at $R=61.2$ cm. This gives an α value of 1.04. Typically the uncertainty in α arising from finite bandwidth of the channel is ± 0.15 in our case. Clearly this will depend both on the channel bandwidth and on α . For very peaked profiles (large α) the uncertainty is greater. Using these values for α during density increase and decrease, respectively, the average densities are calculated at the cutoff times. These calculated average densities are plotted in Fig. 6 together with the average density measured along a central vertical chord through $R=55.7$ cm by a 2 mm interferometer. The vertical error bars on the points in Fig. 6 are due to the uncertainty in α and the cutoff radius due to the finite frequency bandwidth of each channel. The agreement between the average density measured with the 2 mm interferometer and ECE cutoffs is good. During fast density changes fringe hops can occur in the interferometer measurement. These 2π discontinuities in phase are relatively infrequent and rather easy to recognize. They are correlated with

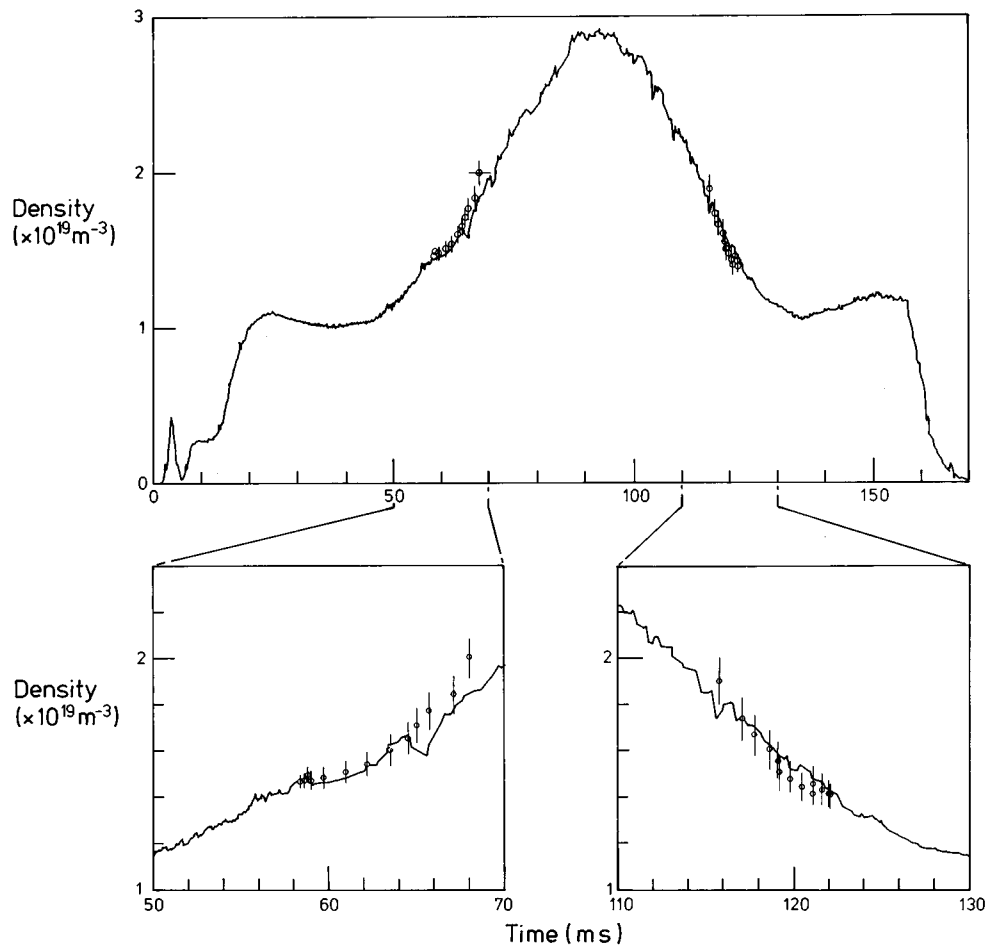


FIG. 6. Evolution of line average plasma density from a 2 mm interferometer and the line average density deduced from the ECE cutoffs.

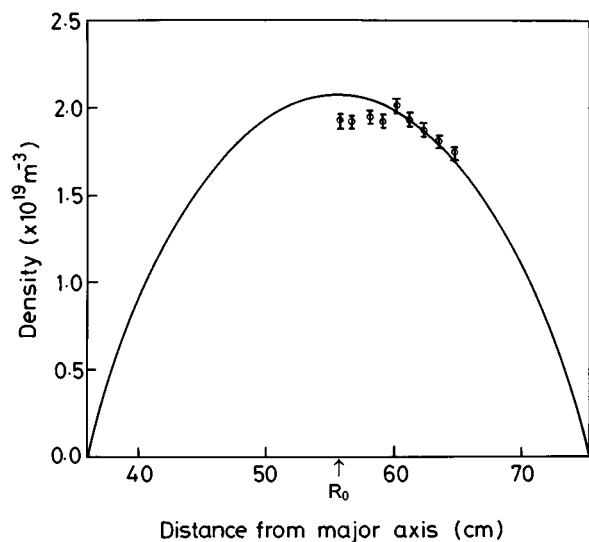


FIG. 7. Radial density profile (solid curve) for $\alpha=0.81$, obtained from the first cutoff frequency. The circles are the values obtained from the cutoffs of individual channels.

a reduction in the fringe amplitude which is also digitized. A computer program which also involves manual checking has been used to remove the “fringe hops” from the interferometer record. Hence the phase change as seen by the interferometer has an uncertainty of about ± 1 fringe (with $\approx 2.6 \times 10^{18} \text{ m}^{-3}/\text{fringe}$). The deviation between the average density calculated from ECE cutoffs and the interferometer has to be viewed in this light and the ECE cutoff density measurement is probably a more reliable measurement during this time.

For typical values of edge densities in COMPASS-C ($\approx 2.5 \times 10^{18} \text{ m}^{-3}$, measured by a reciprocating Langmuir probe) the value of α calculated using Eq. (20) differs from that calculated using Eq. (8) by about 0.1. The line average densities obtained from ECE cutoffs (Fig. 6) would increase by less than 5% as a result of correcting for the finite edge density. However, in certain types of discharges (e.g., *H* mode), where the edge densities are higher and the profiles are broader (smaller α) the difference may be significant.

From the observed ECE cutoffs and the interferometer data, we have obtained the densities at the time of the cut off of frequencies on the low field side (which are local cutoffs) using Eq. (16). These calculated densities representing a part of the profile are shown in Fig. 7 as circles. Though we have only a few points, in principle the whole of the outer density profile could be reconstructed in this way. As mentioned earlier, no explicit form for the density profile needs to be assumed in this way of density profile reconstruction. The solid curve in Fig. 7 represents the profile defined by Eq. (5) with $\alpha=0.81$, which is the value obtained from the first cutoff. The agreement between the data points and the profile obtained from the first cutoff is an absolute one in that no curve fitting or normalization is used.

IV. DISCUSSION

The cutoffs observed by the ECE diagnostic do not occur instantaneously (see Fig. 5). Some of the reasons for this

smearing out are (a) the finite frequency bandwidth of the channels, (b) the cutoff in a plasma occurs over a distance comparable to that of the wavelength, (c) the finite beam width due to the antenna pattern, and (d) the radiation reaching the antenna after reflection from the wall and cutoff layers. We have chosen, arbitrarily, the cutoff occurrence time as the time when the rate of change in the signal is greatest. The uncertainty in the precise instant of cutoff leads to an error which is indicated by the horizontal error bar in Fig. 6. In a multichannel ECE system, if the first channel to cut off is the lowest or the highest frequency channel available then only an upper or lower bound can be put on the value of α .

The methods described in this paper are useful only if the density profile can be parametrized adequately with few parameters. If two free parameters are chosen, the first cutoff condition can be used to calculate both parameters uniquely. If there are three parameters then one independent measurement apart from the ECE cutoffs is required to determine all three parameters.

The technique described in this paper is an independent method for determining the absolute density with no more than a frequency calibration required. During cutoffs, when the ECE diagnostic is not useful for temperature measurement, this technique extends the utility of the diagnostic to obtain valuable information regarding the density profile. Unlike temperature measurements using ECE, the density measurement does not require the plasma to be optically thick.

The densities obtained from the ECE cutoffs are found to be in good agreement with those from an independent interferometric density measurement. Alternatively, the profile on the low field side can be determined using the local cutoffs without assuming any explicit form for the profile. Of course, both these techniques are useful only if the density is large enough to cut off the emission. O-mode fundamental emission is cut off at lower densities and could in principle be used for density measurement at densities lower than those at which the X-mode second harmonic is cut off.

ACKNOWLEDGMENTS

The authors would like to thank B. J. Parham for his help in interpreting the 2 mm interferometer data and Dr. B. Lloyd and T. N. Todd for their helpful comments and suggestions. The authors would like to acknowledge the many helpful suggestions made by the referee. This work was funded jointly by the UK Department of Trade and Industry and Euratom.

¹D. V. Bartlet, D. J. Campbell, A. E. Costley, S. Kissel, N. Lopes Cardozo, C. W. Gowers, S. Nowak, Th. Oyevaar, N. A. Salmon, and B. J. Tubbing, Proceedings of Sixth Joint Workshop on Electron Cyclotron Emission (ECE) and Electron Cyclotron Resonance Heating (ECRH), Oxford, 1987 (unpublished), p. 137.

²G. Taylor, A. Cavallo, P. C. Efthimion, and F. J. Stauffer, in Ref. 1, p. 89.

³S. K. Guharay, D. A. Boyd, R. F. Ellis, F. J. Stauffer, and C. J. Lasnier, Rev. Sci. Instrum. **61**, 3520 (1990).

⁴S. Ishida, A. Nagashima, M. Sato, N. Isei, and T. Matoba, Rev. Sci. Instrum. **61**, 2834 (1990).

⁵A. M. Zolfaghari, S. Luckhardt, P. P. Woskov, D. R. Cohn, S. Jones, J. Kesner, J. Machuzak, J. J. Ramos, D. V. Bartlet, A. E. Costley, P. Crippwell,

- L. Porte, R. J. Smith, and R. Kaita, *Rev. Sci. Instrum.* **63**, 4619 (1992).
- ⁶M. Kown, R. F. Gandy, C. E. Thomas, and W. K. Lim, *Rev. Sci. Instrum.* **63**, 4633 (1992).
- ⁷H. J. Hartfuss and M. Tutter, *Rev. Sci. Instrum.* **56**, 1703 (1987).
- ⁸N. A. Salmon, D. V. Bartlet, and A. E. Costley, in Ref. 1, p. 157.
- ⁹F. F. Chen, *Introduction to Plasma Physics* (Plenum, New York, 1974), p. 112.
- ¹⁰J. Lohr, *Rev. Sci. Instrum.* **59**, 1608 (1988).
- ¹¹R. J. Hayward, P. J. Crawley, R. T. Crossland, B. S. Ingram, A. P. Pratt, and R. T. C. Smith, *Proceedings of the 15th Symposium on Fusion Technology*, Utrecht, The Netherlands, 1988 (unpublished), p. 361.